Journal of Cellular Biochemistry 99:575–588 (2006)

ARC Protects Rat Cardiomyocytes Against Oxidative Stress Through Inhibition of Caspase-2 Mediated Mitochondrial Pathway

Yi-Qiang Zhang and Brian Herman*

Department of Cellular and Structural Biology, University of Texas HSC at San Antonio, 7703 Floyd Curl Dr, San Antonio, Texas 78249

Abstract Apoptosis repressor with a CARD domain (ARC) has been demonstrated to protect heart cells against ischemia/reperfusion (I/R) injury. In this study, we investigated the mechanism by which ARC protects heart cells against oxidative stress. We monitored the extent of apoptosis and activity of multiple components of the intrinsic apoptotic pathway in rat cardiac myoblast cell line H9c2 with either reduced or increased expression of ARC during oxidative stress. Overexpression of ARC-inhibited oxidative stress-induced caspase-2/3 activation, cytochrome c release, and translocation of Bax to mitochondria. Furthermore, phosphorylation of ARC at threonine 149 was found to be critical to its function. ARC containing a T149A mutation failed to translocate to mitochondria, did not inhibit caspase-2 activation, and had a dominant negative effect against the protective effect of endogenous ARC during oxidative stress. In addition, wild-type ARC but not the T149A mutant inhibited cell death induced by overexpression of caspase-2. Using a yeast two-hybrid (YTH) screening approach and co-immunoprecipitation (Co-IP), we found that protein phosphatase 2C (PP2C) interacted with ARC and that PP2C mediated-dephosphorylation of ARC inhibited its anti-apoptotic activity. Eliminating either the N-terminal CARD domain or the C-terminal P/E domain also abolished the anti-apoptotic function of ARC, suggesting that full-length ARC is required for its apoptotic inhibition. These results indicate that ARC plays an important role in protection of H9c2 cells against oxidative stress-induced apoptosis by phosphorylation-dependent suppression of the mitochondria-mediated intrinsic pathway, partially initiated through the activation of caspase-2.
J. Cell. Biochem. 99: 575–588, 2006.

Key words: ARC; oxidative stress; apoptosis; caspase; mitochondria

Oxidative stress-induced apoptosis has been implicated in various tissue injuries including heart and brain ischemia/reperfusion (I/R) injury [Fliss and Gattinger, 1996; Holly et al., 1999; Zhao et al., 2001; Lundberg and Szweda, 2004; Mronga et al., 2004]. Either endogenous or exogenous reactive oxygen species (ROS) can induce apoptosis, and mitochondria are one of the major sources for the generation of endogenous ROS. Under normal physiological conditions, anti-ROS defense systems detoxify ROSs before they can damage cellular structures. One important ROS detoxifying enzyme in mitochondria is magnesium-dependent superoxide dismutase (MnSOD). Eliminating MnSOD has been shown to increase sensitivity of cells to oxidative stress while overexpression enhances their resistance [Van Remmen et al., 1999, 2001; Ran et al., 2003, 2004; Chen et al., 2004]. It appears that cells exposed to oxidative stress die via the intrinsic apoptotic pathway. Recent data further indicate that oxidative stress-induced apoptosis is likely mediated at least partially through caspase-2 activation via the mitochondrial pathway [Araya et al., 1998; Troy and Shelanski, 2003; Takahashi et al., 2004; Qin et al., 2004].

Cell death and survival is fine-tuned at multiple points of the apoptotic pathway by a variety of mechanisms. One major regulatory mechanism is to control the activation and/or

Grant sponsor: NIH; Grant number: AG20210; Grant sponsor: NIA; Grant number: AG021890.

*Correspondence to: Brian Herman, Department of Cellular and Structural Biology, University of Texas HSC at San Antonio, 7703 Floyd Curl Dr., San Antonio, TX 78249.
E-mail: hermanb@uthscsa.edu

Received 12 January 2006; Accepted 13 March 2006
DOI 10.1002/jcb.20946

activity of caspases in the apoptotic pathways [Deveraux et al., 1999; Nicholson, 2001]. One example of such regulation is the inhibitors of apoptosis protein (IAP) family of caspase inhibitors, which bind and inhibit activated forms of caspases with relative specificity for specific caspases [Deveraux and Reed, 1999; Tenev et al., 2005]. Apoptosis repressor with a CARD domain (ARC), similar to IAP, is a pleiotropic apoptosis inhibitor [Koseki et al., 1998; Ekhterae et al., 1999; Neuss et al., 2001]. It inhibits both the intrinsic and the extrinsic apoptotic pathways in H9c2 cells by either directly binding to caspase-2 and -8 or indirectly preserving the integrity of mitochondria [Gustafsson et al., 2004; Nam et al., 2004]. ARC is abundantly expressed in cardiac and skeletal muscle cells and has been shown to inhibit hydrogen peroxide-induced cell death in cardiomyocytes. ARC is phosphorylated at threonine 149, which is important for its translocation to mitochondria and interaction with caspase-8 [Li et al., 2002]. ARC has two domains, the CARD and the P/E (proline/glutamic acid-rich) domain and the role of these domains in ARC remains unknown. In addition, detailed and systemic information about the mechanism of how ARC protects cells against oxidative stress is still lacking. For example, the role of phosphorylation on caspase inhibition by ARC during oxidative stress has not been well studied. Additionally, other uncharacterized cellular proteins may interact with ARC and modulate its function.

In order to understand the role of ARC in oxidative stress-induced apoptosis in cardiomyocytes, we investigated the responses of H9c2 cardiomyocytes to both endogenous and exogenous ROS as a function of ARC expression level, ARC domain structure, and molecular interactions of ARC with other cellular proteins. The yeast two-hybrid (YTH) system was utilized to identify factors that might interact and modulate the action of ARC. The activation/inactivation of several caspases was also investigated. Our data demonstrate that ARC protects H9c2 cells against inducers of both endogenous and exogenous ROS by blocking the mitochondria-mediated intrinsic pathway, particularly the inhibition of caspase-2 activation and the translocation of Bax to mitochondria. The protection requires intact ARC protein and phosphorylation at threonine 149. YTH and co-immunoprecipitation (Co-IP) approach demonstrated that protein phosphatase 2C (PP2C) interacts with ARC and may dephosphorylate ARC, inhibiting its anti-apoptotic activity.

MATERIALS AND METHODS

Cell Culture and Reagents

H9c2 cells were purchased from the ATCC and maintained in Dulbecco's modified Eagle's medium (Life Technologies, Inc.) supplemented with 10% fetal bovine serum. H_2O_2 (30% solution), *tert*-butyl hydroperoxide (70% solution), rotenone, and anti-mycin A were purchased from Sigma. Casein kinase II (CKII) inhibitor, DRB (5,6-dichlorobenzimidazole 1-β-D-ribofuranoside) was purchased from Calbiochem. The caspase inhibitors, z-VAD-FMK (pan caspase inhibitor), z-VDVAD-FMK (caspase-2 inhibitor), z-DEVD-FMK (caspase-3 inhibitor), z-IETD-FMK (caspase-8 inhibitor), and z-LE HD-FMK (caspase-9 inhibitor) were purchased from R&D Systems.

Plasmid Construction and Transfection

ARC, ARC-CARD$_{(1-98)}$, and ARC-P/E$_{(98-208)}$ were amplified by PCR and subcloned into pCMV-Tag (Stratagene) and pECFP$_{N1}$ (Clontech) vectors. Full-length caspase-2 cDNA was amplified by RT-PCR from mouse total RNA and subcloned into pEYFP$_{N1}$ (Clontech). The 30-kDa catalytic domain of caspase-2 was cloned into pEYFP$_{N1}$ using PCR with specific primers. ARC (T149A) and ARC (T149D) were generated by site-directed mutagenesis using pCR2. 1rARC or pcDNA3.1rARC as template and subcloned into pECFP$_{N1}$. Bax was subcloned into pEYFP$_{N1}$ vector. Transfection was carried out with Lipofectamine 2000 (Invitrogen) according to manufacturer's instructions. For transient transfection experiments, H9c2 cells were transfected and incubated for 24 h before treatment. For stable transfection, stable cell clones were generated by selection with 1 mg/ml of G418 or 300 μg/ml of hygromycin for at least 2 weeks after initial transfection and maintained with antibiotics throughout the culturing period. The protein expression was confirmed by fluorescence microscopy and Western Blot analysis. In all experiments stable cell clones were used, except where noticed.

siRNA Design and Transfection

The siRNA oligos specific for rat ARC were designed and synthesized by Qiagen, Inc. Four

siRNA oligoes: rARC1 r(GGUUGUGAGAACAC CUAAA); rARC2 r(CAAGGAGCUCUGUACAU UAUU); rARC3 r(AGAGUAUCAAGCAAGUGA AUU); rARC4 r(CGACUAGACUUAAGAGUA UUU); and scrambled siRNA oligo: r(CGACUA-GAAUUAAAUAUUU) were employed. The cDNA corresponding to the siRNA (rARC4) was synthesized and subcloned into the expression vector pRNAT/Hygro (Genescript, Inc.). Both transient and stable expression of siRNA on ARC expression was tested. For transient expression, siRNA was transfected into H9c2 cells using Oligofectamine according to the manufacturer's instruction (Invitrogen, Inc.). The cells were used for experiments 64 h after initial transfection. For stable expression, siRNA plasmid was transfected into H9c2 cells using Lipofectamine 2000 as described earlier. Stable transfected cell clones were established by hygromycin (300 μg/ml) selection for at least 2 weeks and the culture was maintained in this antibiotic throughout the experiment.

Oxidative Stress and Apoptosis Analysis

H9c2 cells were subjected to different ROS inducers including hydrogen peroxide, *t*-butyl hydroxyl peroxide, rotenone, and anti-mycin A for 0–48 h (depending on the treatment) at specified concentrations as indicated in the legend and results. Cell death was monitored by the following approaches. The MTT assay was used for general analysis of cell viability as previously described [Mc Caughan et al., 1994]. DAPI staining for nuclear condensation/fragmentation was used to monitor apoptosis. Fragmented or condensed nuclei were considered apoptotic. Western Blot analysis of cleaved caspase-3 and/or fluorometric caspase-3 substrate assay (Alexis, Inc.) was used to demonstrate the activation of this caspase. The caspase inhibitors, z-VAD-FMK, z-VDVAD-FMK, z-DE VD-FMK, z-IETD-FMK, or z-LE HD-FMK were applied to examine the participation of different caspases in apoptosis in concentrations specified in the text.

Cell Fractionation

A mitochondria-enriched high molecular weight fraction was isolated following the method of Takeyama et al. [2002]. Briefly, cells were harvested by trypsinization and collected by centrifugation followed by washing with 1× phosphate buffered saline (PBS). Cells were resuspended in cold mitochondria isolation buffer (MIB: 220 mM mannitol, 68 mM sucrose, 10 mM KCl, 1 mM EDTA, 1 mM EGTA, 10 mM HEPES-KOH, pH 7.4, 0.1% BSA, Protease inhibitor cocktail) and homogenized with a Dounce homogenizer for 30 strokes, which was optimized using healthy H9c2 cells and 25 strokes for treated H9c2 cells. The homogenate was centrifuged at 750 × *g* for 5 min at 4°C. The supernatant was transferred to a new tube. The pellet was washed once and the supernatants were combined. The combined supernatant was centrifuged at 10,000 × *g* for 15 min at 4°C. The supernatant from this step contained the cytosolic fraction with low MW membrane fraction. The pellet contained high MW membrane fraction with concentrated mitochondria (S100 fraction). The pellet was further washed twice with MIB to eliminate cytosolic contamination.

Yeast Two-Hybrid and Co-Immunoprecipitation

The YTH kit and heart cDNA library were purchased from Invitrogen. ARC was inserted into vector pDEST32 in frame with the Gal4 DNA binding domain. This plasmid and the cDNA library were co-transformed into the yeast strain MaV203 according to manufacturer's instructions and the library was screened following criteria specified by the kit. The results were compared with five standard strains of yeast to determine the strength of interaction. DNA was isolated from positive clones and sequenced.

Co-IP was performed as follows. H9c2 cells expressing CFP-tagged ARC or ARC-T149A were harvested and lysed with RIPA buffer (1× PBS, 1% Nonidet P-40, 0.5% sodium deoxycholate, 0.1% SDS) containing protease inhibitors on ice. The lysate was centrifuged at 10,000 × *g* for 10 min at 4°C. The supernatant was used for immunoprecipitation. Briefly, the supernatant was incubated with normal rabbit or mouse IgG and agarose beads for 30 min at 4°C to eliminate non-specific binding. After centrifugation at 400*g* for 30 s, the supernatant was transferred to a new tube and incubated with agarose-conjugated anti-GFP antibody (Santa Cruz) overnight at 4°C on a rotary mixer. At the end of incubation, the mixture was centrifuged at 400 × *g* for 1 min followed by four washes with cold 1× PBS. The final precipitate was boiled in sample buffer before loading to SDS–PAGE gel.

Antibodies and Western Blot

The protein concentration of cell lysates was determined using the BCA protein assay reagent (Pierce). Equal amount of protein was loaded onto 12% Tris-glycine SDS–PAGE gel and separated at 100 volts for 1 h. The protein was transferred to PVDF membrane and blocked with 5% milk in TBST buffer. ARC was detected with anti-ARC antibody (Oncogene). Bax was detected with anti-Bax antibody (BD Sciences). Cytochrome c was detected with anti-cytochrome c antibody (BD Sciences). Anti-COX IV (Molecular Probes) and anti-actin (Sigma) antibody was used to quality control of the mitochondrial and cytosolic fractions as well as the equal loading of samples.

Fluorescence Imaging

Cells expressing fluorescence-tagged fusion protein were fixed on cover slips with 4% paraformaldehyde in PHEM buffer (60 mM Pipes, 25 mM Hepes, 10 mM EGTA, 2 mM MgCl2, pH 7.2) for 30 min at room temperature and mounted onto glass slides. When immunofluorescence was required, fixed cells were permeabilized with 0.5% Triton X-100 for 5 min followed by 4×10 min wash with $1\times$ PBS. The slides were covered with specific antibody in 5% PBS and incubated at 37°C for 60 min followed by three washes. The slides were further incubated with fluorescent secondary antibody (Cy5 from Molecular Probes) for 1 h at 37°C followed by four washes. For labeling specific intracellular organelle, either live cell culture or fixed samples were incubated with specific fluorescent markers according to product specification. Fluorescence imaging was performed with either a Zeiss or Olympus confocal fluorescent microscope. For ECFP, the excitation wavelength was 458 nm and emission wavelength is 488 nm. For Cy5, the excitation wavelength was 649 nm and emission at 670 nm.

Fluorescence resonance energy transfer (FRET) is a distance-dependent interaction between the electronic excited states of two dye molecules in which excitation is transferred from a donor molecule to an acceptor molecule without emission of a photon. FRET was detected by the acceptor photo-bleaching approach using a Zeiss LSM510 laser scanning confocal microscope as described previously [Herman et al., 2004]. The donor (ECFP) filter set consisted of (excitation (ex) = 480–500 nm; dichroic mirror (dm) = 510 nm; emission (em) = 515–555 nm). The acceptor (EYFP) filter set consisted of (ex = 546/40 nm; dm = 580 nm; em = 590 nm long pass). The FRET filter set consisted of (ex = 450–490 nm; dm = 580 nm; em = 580 long pass). The signal recorded from this filter set is the FRET signal that arises from energy that has been transferred from ECFP to EYFP molecules.

Statistical Analysis

Data are expressed as the mean ± SEM. The significance of differences between values was analyzed by either one-way or two-way ANOVA. For each time point or experiment, triplicate or quadruplicate samples were analyzed. A P-value of <0.05 was considered statistically significant.

RESULTS

Inhibition of ARC by siRNA Increases Sensitivity of H9c2 Cells to Oxidative Stress

First, the level of ARC expression in H9c2 cells following treatment with ARC-specific siRNA was examined. Two siRNA oligos (#3 and #4 siRNA) were found to inhibit the expression of ARC effectively. As shown in Figure 1A, 60 h after introducing ARC-specific siRNA, ARC protein level was reduced significantly: over 50% reduction when compared to the control (the right lane). The corresponding siRNA cDNA (#4) was also inserted into pRNAT-CMV/Hygro vector for stable expression. Several stable cell clones were generated by hygromycin selection. As shown in Figure 1B, ARC expression in stable cell clone #3 and #5 was reduced significantly (~70%) compared to cells with only vector or scrambled siRNA. The reduction of ARC protein expression appeared to be greater in stable cell lines than that obtained using transient transfection.

After confirming the reduction of ARC expression, the sensitivity of these cells to oxidative stress-induced cell death was examined. H9c2 cells transfected with ARC-specific siRNA and control siRNA were treated with hydrogen peroxide (200, 400 μM) for 24 h. The cells were either analyzed for viability using MTT assay or stained with DAPI for nuclear condensation and fragmentation. As shown in Figure 1C, ARC-specific siRNA dramatically increased the sensitivity of H9c2 cells to hydrogen peroxide. DAPI staining demonstrated specific apoptotic

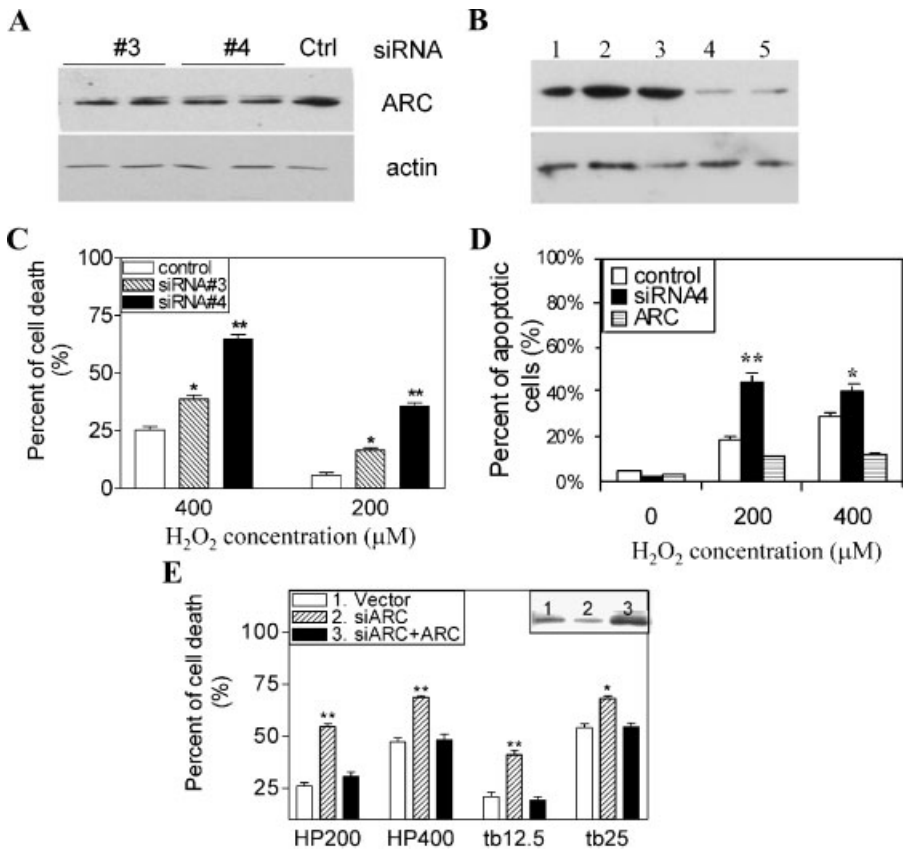

Fig. 1. The ARC-specific siRNA oligos reduced the resistance of H9c2 cells to oxidative stress. **A**: Western Blot analysis of transient-transfected H9c2 cells with siRNA-rARC. **Lanes 2** and **3**: ARC-siRNA #3, **lanes**3 and **4**: ARC-siRNA #4, **lane 5**: control siRNA. **B**: Western Blot analysis of stable cell clones with ARC-siRNA #4. **Lane 1**: control siRNA clone, lanes 2 and 3: scrambled siRNA clones, lanes 4 and 5: independent ARC-siRNA clones. **C**: Cell viability analysis using MTT assay as described in Materials and Methods. H9c2 cells were transiently transfected with either ARC-siRNA #3 or #4 for 48 h followed by treatment with hydrogen peroxide for 24 h. Data were statistically significant ($^*P < 0.05$ between #3 and control; $^{**}P < 0.01$ between #4 and control). **D**: H9c2 cells died through apoptosis. H9c2 cells transfected with vector, ARC, or siRNA #4 (stable clone) were stained with propidium iodide (100 nM) after hydrogen peroxide (400 μM, 12 h) treatment. Cells with condensed or fragmented nucleus were considered apoptotic cells. Two-hundred cells were counted in total. Percent of cell death was calculated as number of apoptotic cells divided by total number of cells. **E**: Reintroduction of wild-type ARC into H9c2 cells that stably expresses ARC-specific siRNA restores resistance against oxidative stress. The inlet graph indicates the expression level of ARC in cell lines used in this experiment. Cells were treated with either hydrogen peroxide (200 and 400 μM) or tBOOH (12.5 and 25 μM) for 24 h followed by MTT assay. Data were significant ($^*P < 0.05$ for tb25, $P < 0.01$ for HP200, HP400, and tb12.5).

characteristics like nuclear condensation and fragmentation (data not shown). The percentage of apoptotic cells with condensed or fragmented nuclei is shown in Figure 1D. There was a significant increase in the number of apoptotic cells when ARC expression was reduced by specific siRNA compared to that of the control cells.

To understand whether the decrease of resistance in siRNA expressing cells is due to the reduction of ARC rather than other non-specific events, wild-type ARC was reintroduced into H9c2 cells with stably expressed ARC-specific siRNA. As shown in Figure 1E, reintroduction of wild-type ARC into cells that are stably expressing ARC-specific siRNA restored resistance against oxidative stress to the same or even a slightly higher level, indicating the decrease of resistance was caused by the reduction of ARC. Since siRNA targets the 3′ UTR of ARC, it does not affect the reintroduced wild-type ARC that lacks the 3′ UTR.

ARC Protects Cells From Oxidative Stress-Induced by Variety of ROS

Oxidative stress can be induced by variety of ROS from both exogenous and endogenous sources. We have examined the effect of ARC on hydrogen peroxide and *t*-butyl hydroxyl

peroxide earlier, which are exogenously sources. However, in physiological conditions, there are a variety of endogenously generated ROS with one major source being the respiratory chain in mitochondria. It has been shown that inhibition of either complex I (by rotenone) or complex III (by anti-mycin A) will generate ROS and induce apoptosis. Therefore, we compared the capacity of ARC to protect cells against both endogenous and exogenous ROS-induced apoptosis. We first normalized the concentration of different ROS inducers such that they would induce apoptosis in H9c2 cells. As confirmed earlier, hydrogen peroxide at 200–400 μM and tBOOH at 12.5–25 μM induced apoptosis (Fig. 1D). Rotenone and anti-mycin A also induced apoptosis in H9c2 cells at concentrations from 5 to 10 μM and 10 to 25 μg/ml, respectively. As indicated in Figure 2A, reduction of endogenous ARC significantly increased sensitivity against ROS from both endogenous (rotenone and anti-mycin A) and exogenous (hydrogen peroxide) sources. These data indicate that ARC has profound role in protection against various sources of oxidative stress.

Effect of Different Domains and Phosphorylation of ARC in Oxidative Stress-Induced Apoptosis

It has been shown that phosphorylation is important for the translocation of ARC to mitochondria where it interacted with caspase-8 [Li et al., 2002], but its role in ARC protection against oxidative stress-induced apoptosis has not been investigated. In addition, ARC contains a CARD domain at the N′-terminus and a proline–glutamine (P/E) rich region in the C′-terminus which has been shown to interact with other proteins involved in apoptosis. However, the role of each domain in oxidative stress-induced apoptosis was not examined. This study examined the role of both phosphorylation and domain structures of ARC in oxidative stress-induced apoptosis. First, the phosphorylation site threonine 149 was mutated to either alanine (T149A) or aspartic acid (T149D). Alanine mutation led to the loss of phosphorylation capability and aspartic acid mimicked constitutive phosphorylation. The CARD and P/E domains were subcloned separately into vectors as described in the Materials and Methods section. H9c2 cells transfected with these constructs were tested for sensitivity to oxidative

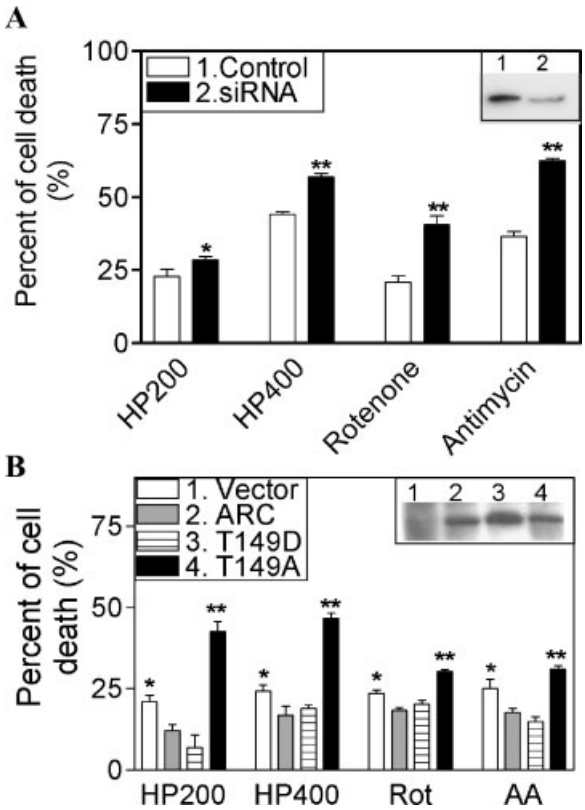

Fig. 2. ARC protects H9c2 cells against variety of ROS inducers. H9c2 cells were treated with H_2O_2 (200 and 400 μM) or tBOOH (12.5 and 25 μM) for 24 h, with rotenone (10 μM) or anti-mycin (25 μg/ml) for 48 h. Cell viability was analyzed by MTT assay as described in Materials and Methods. **A**: Reduction of endogenous level of ARC increases sensitivity to both endogenous and exogenous ROS. H9c2 cells stably expressing ARC-siRNA (siRNA #4) or vector alone were treated with ROS. (*$P < 0.05$) (**B**) Compare T149A, T149D mutant of ARC in H9c2 cells against various ROS. The result was generated from stable cell lines expressing individual protein as specified. Data are statistically significant (*$P < 0.05$, **$P < 0.01$). The inlet graph indicates the expression of ARC in stable cell lines used in the experiment. All experiments were performed at least three times.

stress. Figure 3A shows that after treatment with hydrogen peroxide, a higher number of ARC-T149A expressing cells exhibit a diffused pattern of cytochrome c staining compared to cells expressing wild-type ARC. Cell viability assays, shown in Figure 2B and 3B, indicate that the T149A mutation significantly decreased resistance of H9c2 cells to hydrogen peroxide (75% cell death compared to 60% for control cells and 50% for cells overexpressing ARC). In contrast, the constitutive phosphorylation mutant (T149D) significantly enhanced resistance against oxidative stress even greater than wild-type ARC (Fig. 2B). Furthermore, wild-type ARC inhibited the release of cytochrome c

significantly more than either the CARD or P/E domains alone. Figure 3B also demonstrates that neither the CARD nor the P/E domain alone protected H9c2 cells against oxidative stress. Additionally, when both domains were expressed together in the same cell but in separate constructs, no protection was observed either (data not shown), indicating correctly folded CARD and P/E domains of intact ARC protein are required for the protective effect of ARC.

The importance of Thr149 was further investigated. Since it has been shown that CKII can phosphorylate ARC at Thr149 [Li et al., 2002], we tested whether inhibition of Thr149 phosphorylation could alter the sensitivity of H9c2 cells to oxidative stress. H9c2 cells stably transfected with different ARC constructs were treated with the CKII inhibitor DRB at 25–75 μM for 48 h before challenged with 200 or 400 μM hydrogen peroxide. As shown in Figure 3C, when there was no DRB treatment, overexpression of ARC protected H9c2 cells relative to either control or the T149A mutant, consistent with earlier observations. However, when cells were treated with DRB, overexpression of ARC did not protect the cells, indicated by the similar level of cell death in all three groups of cells. At the tested concentration, DRB did not affect the cell viability (data not shown). This data indicates that phosphorylation of ARC is critical for protecting cells from oxidative stress-induced damage.

The localization of different ARC constructs in H9c2 cells was also investigated (Fig. 3E). A significant amount of wild-type ARC was colocalized with mitochondria in response to oxidative stress, indicated by the yellow color in the overlay image. However, neither ARC (T149A) nor the CARD or P/E domains alone colocalized significantly with mitochondria under either normal or oxidative stress conditions. Western Blot analysis (Figs. 3D and 5D) further indicates that phosphorylation at Thr149 is required for the translocation of ARC to mitochondria as has been previously demonstrated [Li et al., 2002].

Identification of PP2C (PPM1G) That Interacts With ARC

To identify potential ARC interacting partners, the YTH system was used to screen a heart cDNA library for new proteins that might interact with ARC. As shown in Table I, several genes were identified by YTH with interactions ranging from weak to strong, as judged by the intensity of the color from β-galactosidase assay (Fig. 4A). Of these genes, one named PPM1G (also known as PP2C), is of particular interest due to its dephosphorylation activity. PP2C is a serine/threonine phosphatase [Flajolet et al., 2003]. The interaction of PP2C with ARC suggests that PP2C might regulate ARC by dephosphorylation at threonine 149. To confirm the interaction between ARC and PP2C, Co-IP was performed. Cells expressing ARC-CFP fusion proteins were immunoprecipitated with anti-GFP antibody and blotted with anti-PP2C antibody as well as anti-ARC antibody. As indicated in Figure 4B, PP2C was co-immunoprecipitated with anti-GFP antibody in cell lysates from wild-type ARC expressing cells but not from T149A expressing cells.

ARC Inhibits Oxidative Stress-Induced Apoptosis by Blocking Caspase-2 Activation and Bax Translocation

To analyze further the mechanism of how ARC affects oxidative stress-induced apoptosis in H9c2 cells, we used stable H9c2 cell lines expressing either siRNA-ARC or wild-type ARC and monitored the activation of various caspases. As shown in Figure 5A, caspase-2 and -3 were activated in H9c2 cells challenged with hydrogen peroxide. This activation was inhibited by overexpression of wild-type ARC but not by overexpression of the phosphorylation mutant (T149A), truncated ARC, or reduced ARC expression by siRNA.

As shown in Figure 5B, inhibitors of caspase-2, -3, -9 or pan caspase inhibitors partially blocked cell death due to the decrease of ARC expression. This effect is similar to the effect of overexpression of ARC. Figure 5B also indicates that the caspase inhibitors have a synergistic effect with overexpression of wild-type ARC, but not the phosphorylation mutant. Inhibition of caspase-2 was more effective than inhibition of caspase-9. This data suggest that caspase-2 might be a major initiator caspase during ROS-induced apoptosis in H9c2 cells and ARC protects H9c2 cells by inhibiting the activation of caspase-2. Inhibitors for caspase-8, either z-LETD-FMK or z-IETD-FMK (more specific for caspase-8) did not block cell death under the similar condition. The result of z-IETD-FMK studies is shown in Figure 5C.

ARC overexpression also blocked the cleavage of caspase-3 and the translocations of Bax to

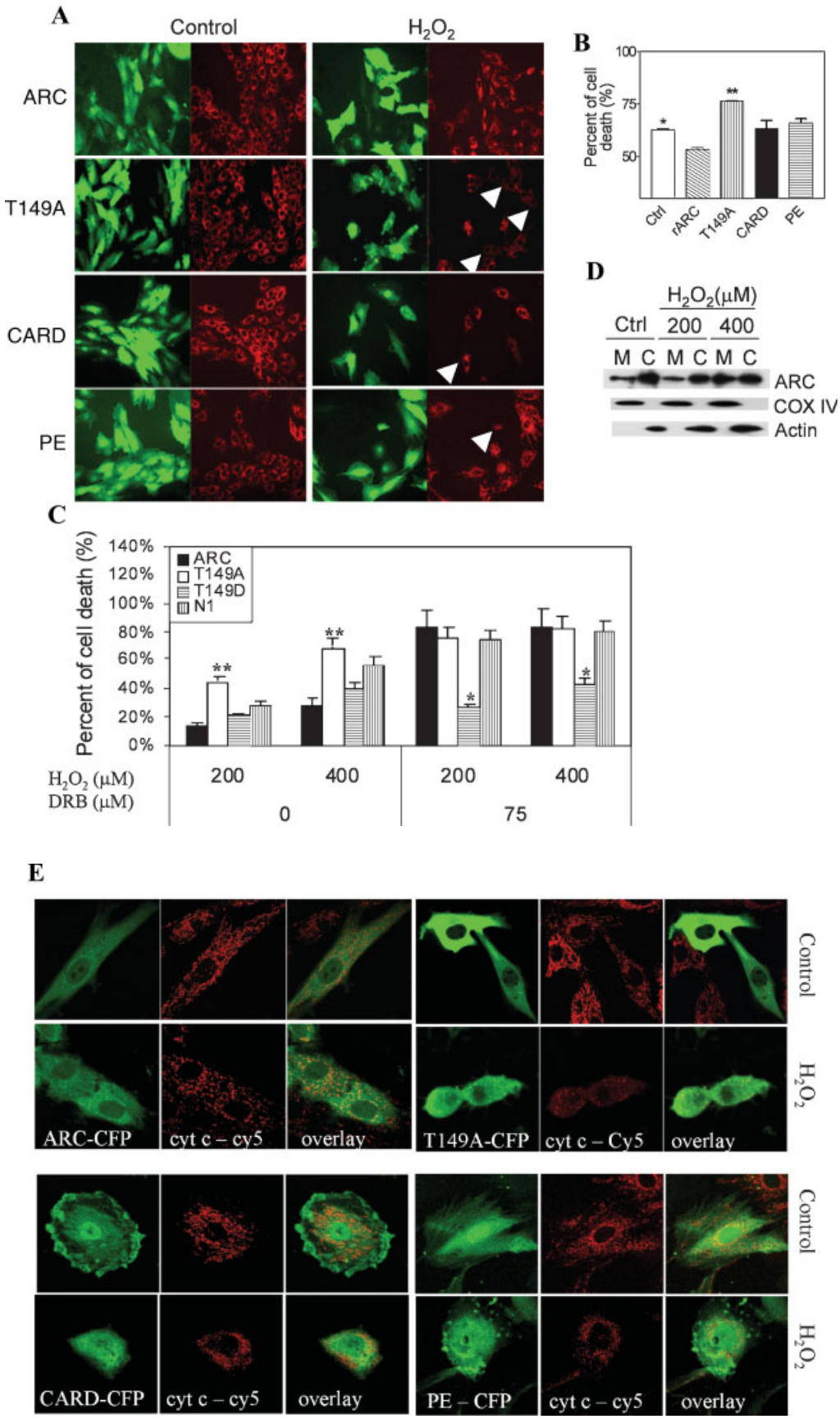
A
Control
H2O2
ARC
T149A
CARD
PE
B
Percent of cell death (%)
100
75
50
*
**
Ctrl
rARC
T149A
CARD
PE
D
H2O2(μM)
Ctrl
200
400
M C M C M C
ARC
COX IV
Actin
C
Percent of cell death (%)
140%
120%
100%
80%
60%
40%
20%
0%
ARC
T149A
T149D
N1
**
**
*
*
H2O2 (μM)
DRB (μM)
200
400
200
400
0
75
E
Control
H2O2
ARC-CFP
cyt c – cy5
overlay
T149A-CFP
cyt c – Cy5
overlay
Control
H2O2
CARD-CFP
cyt c – cy5
overlay
PE – CFP
cyt c – cy5
overlay

Fig. 3.

TABLE I. Example of Proteins that Might Interact with ARC Identified by YTH

Clone	Gene	Interaction
1a, 5a, 7a, YTH20	ARC	Moderate
d14	*PPM1G (PP2C)*	Weak
d18	Mitochondrial unknown gene	Weak
d26	RNA binding protein	Weak
d8	Kazrin	Strong

mitochondria as shown in Figure 5D (top panel). ARC was detected in mitochondria-enriched fraction isolated from wild-type ARC overexpression cells, but no phosphorylation mutant ARC (T149A) was detected from mitochondrial fraction isolated from T149A overexpressing cells. This is consistent with our earlier findings using fluorescence microscopy (Fig. 3B). Significantly, more Bax was detected in the mitochondrial fraction from cells expressing T149A mutant but not in cells overexpressing wild-type ARC (second panel). Furthermore, caspase-3 was cleaved into 19-kDa fragments to a greater degree in T149A-transfected cells than in cells overexpressing wild-type ARC (third panel). These data indicate that the inhibition of oxidative stress-induced apoptosis by ARC occurred through inhibition of the mitochondrial pathway of apoptosis.

The interaction between ARC and Bax was further analyzed by FRET. As indicated in Figure 5E, when wild-type ARC and Bax were co-expressed in the same cell, an increase of FRET efficiency after ROS treatment was observed. However, when T149A mutant of ARC and Bax were co-expressed in the same cell, no changes in FRET efficiency was observed after ROS treatment. Furthermore, the basal FRET efficiency for T149A mutant and Bax is barely detectable, suggesting no interaction exists between T149A mutant and Bax under any tested conditions, further supporting our findings displayed in Figure 5D.

ARC Blocks Cell Death Induced by Overexpression of Full-Length Caspase-2

Caspases have been shown to induce apoptosis when overexpressed in cells [Baliga et al., 2004; Gao et al., 2005]. Here, we tested whether ARC could block cell death induced by overexpression of caspase-2. Stable H9c2 cells expressing different ARC constructs (ARC, T149A mutant, CARD, and P/E domain) were transiently transfected with either full-length caspase-2 (casp2-FL) or caspase-2 without pro-domain (casp2-Cat). Cell viability was measured using the MTT assay. As shown in Figure 6A, wild-type ARC inhibited apoptotic cell death due to overexpression of full-length caspase-2 (left panel of Fig. 6A), but not the catalytic domain of caspase-2 which lacks the pro-domain (right panel of Fig. 6A). In contrast, the T149A mutant did not inhibit cell death induced by overexpression of either full-length or catalytic domain of caspase-2. On the contrary, it interfered with endogenous ARC, leading to more cell death compared with control cells. Expression of the CARD or PE domain separately had similar effect as that of control cells, indicating a requirement for full-length, intact ARC to inhibit caspase-2 activation. This is consistent with the notion that ARC inhibits caspase-2 by interacting through the CARD domain localized in the pro-domain of caspase-2. The binding of ARC to caspase-2 was examined further by Co-IP. As shown in Figure 6B, wild-type ARC co-immunoprecipitated with caspase-2, but not T149A

Fig. 3. Effect and localization of different domains of ARC in H9c2 cells against oxidative stress-induced cell death. **A**: H9c2 cells expressing different ARC-CFP fusion constructs were treated with 200 μM H_2O_2 for 12 h before fixation. The cells were further immunostained with antibody specific for cytochrome c and labeled with Cy5-conjugated secondary antibody. The image was taken using Olympus wide field laser microscope. **B**: H9c2 cells stably transfected with constructs of different ARC domains or mutants were treated with 400 μM H_2O_2 for 24 h. Cell viability was analyzed by MTT assay as described in Materials and Methods. Data are statistically significant (*$P < 0.05$ between control and T149A, **$P < 0.01$ between ARC and T149A). **C**: Inhibition of phosphorylation in ARC with CKII inhibitor DRB reduces resistance of H9c2 cells against oxidative stress. Cells were pretreated with DRB for 48 h before treated with H_2O_2 for another 24 h. Cell viability was analyzed by MTT assay (*$P < 0.05$ between control and T149A, **$P < 0.01$ between ARC and T149A). **D**: Detect translocation of ARC to mitochondria using Western Blot analysis. Mitochondria were isolated as described in the Materials and Methods. ARC was detected with antibody specific for hARC (1:1,000). Mitochondrial and cytosol fraction were probed with antibodies specific for COX IV and β-actin respectively. Ctrl, control. **E**: Analyze the localization of ARC protein using fluorescence microscope. H9c2 cells stably transfected with respective ECFP fusion constructs were treated with or without H_2O_2. Mitochondria were labeled with anti-cytochrome c antibody (Cy-5 conjugated secondary antibody). Green fluorescence indicates ARC protein, read fluorescence cytochrome c. Yellow color indicates co-localization of read and green signals.

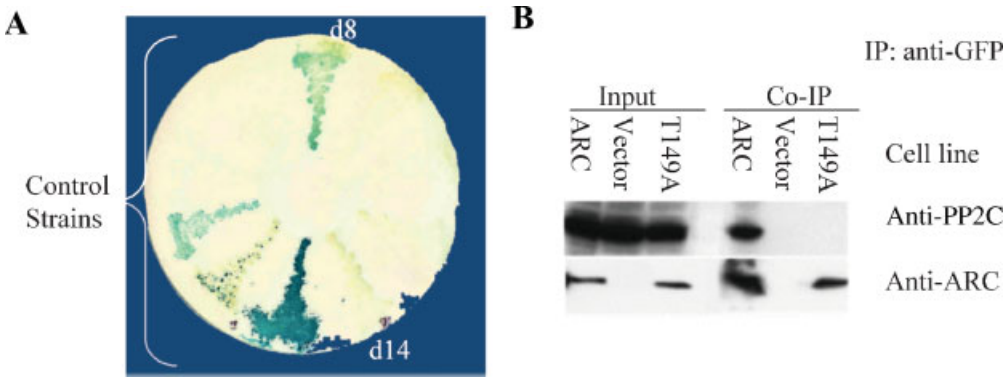

Fig. 4. Identification of PP2C as a potential protein phosphatase to dephosphorylate ARC. **A**: β-galactosidase assay of YTH clones. Control strains are standard yeast strains provided by Invitrogen, with interaction strength from weak to very strong (indicated by no color to deep blue color). YTH clones screened from heart cDNA library were labeled as d8, d14, d15, d18, and d26. **B**: Co-immunoprecipitation (Co-IP) experiment confirms the interaction between ARC and PP2C. ARC was precipitated with anti-GFP antibody and PP2C was detected with anti-PP2C antibody following immunoprecipitation.

mutant, suggesting that phosphorylation of ARC at threonine 149 is also important for interaction between ARC and caspase-2.

DISCUSSION

In this study, we investigated in detail the mechanism by which ARC protects rat H9c2 cardiomyocytes against oxidative stress-induced apoptosis. Specifically, we focused on the level of expression, phosphorylation, and the domain structure of ARC in protection against oxidative stress-induced apoptosis. We also explored the relationship either between ARC and caspase activation or between ARC and Bax translocation during oxidative stress. The results indicate that a high level of expression of ARC and the maintenance of ARC protein level inside H9c2 cells is critical to their protection against oxidative stress-induced apoptosis. When ARC expression was reduced by ARC-specific siRNA, H9c2 cells were significantly more sensitive to oxidative stress. In contrast, overexpression and maintenance of high levels of ARC in H9c2 cells significantly increased resistance to oxidative stress. Individual domains of ARC had no protective effect when overexpressed separately in H9c2 cells, indicating that the integrity of the whole ARC protein structure is important. Most importantly, phosphorylation of ARC at threonine 149 is critical to its anti-apoptotic function. When this phosphorylation site was eliminated (threonine → alanine), ARC had a dominant negative effect on endogenous wild-type ARC. The importance of phosphorylation was further confirmed by a constitutive phosphorylation mimicry mutation (threonine → aspartic acids) which protected H9c2 cells even more than wild-type ARC. When phosphorylation at threonine 149 was inhibited pharmacologically, protection also decreased. Further investigation disclosed that T149 is critical for the translocation of ARC to mitochondria. Wild-type ARC inhibits the translocation of Bax to mitochondria, the release of cytochrome c from mitochondria, and activation of caspase-3. However, a mutation of T149A resulted in loss of all of these properties. Using the YTH system, we discovered that PP2C interacts with ARC. In addition, we found that caspase-2 inhibitors had synergistic effects with ARC in blocking oxidative stress-induced apoptosis. When the ARC level was reduced by siRNA, caspase-2 activity was significantly higher than that in those cells with normal levels of ARC, suggesting ARC under normal conditions can suppress the activation of caspase-2.

We have made several new findings in this study. First, using ARC-specific siRNA, we found that the level of ARC is critical to the protection of H9c2 cells against oxidative stress. Second, the integrity of the ARC protein is required for its anti-oxidative stress function; expression of either domain alone did not protect cells against oxidative stress. Third, phosphorylation is crucial for ARC to be protective. Mutant ARC that could not be phosphorylated had dominant negative effects against endogenous ARC. A newly identified

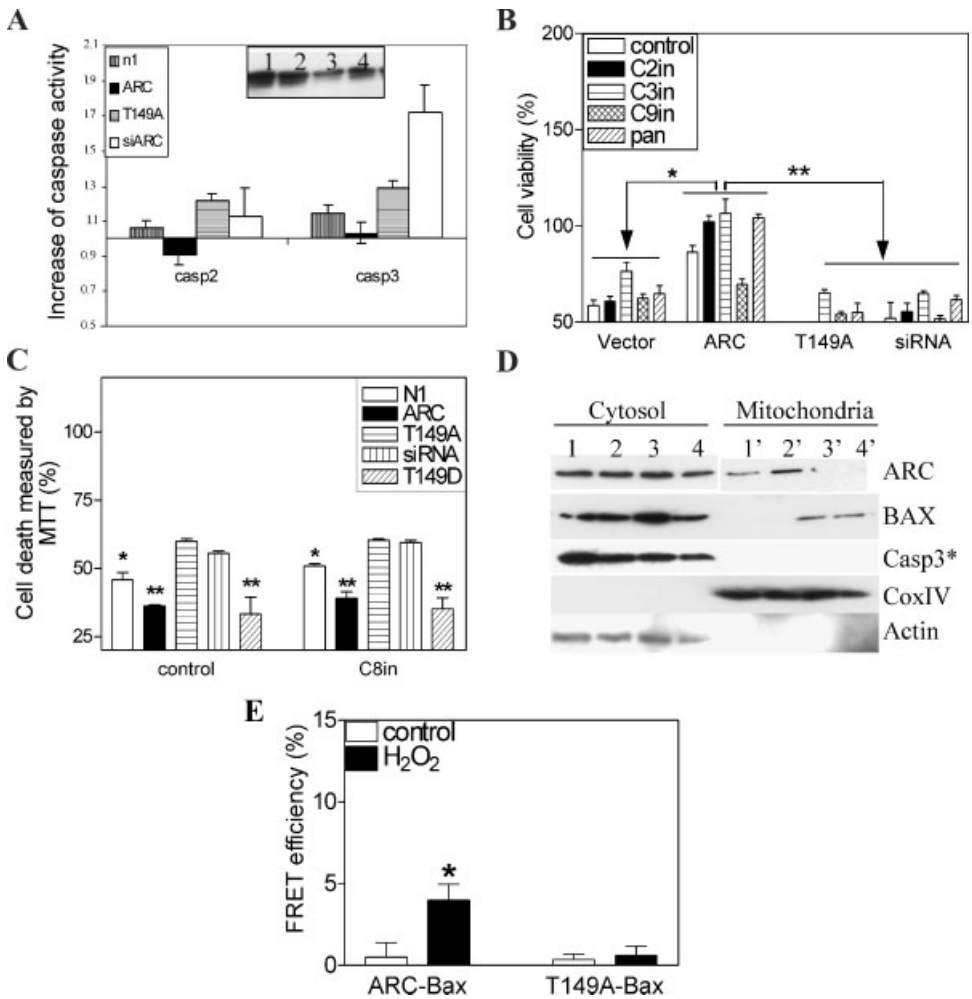

Fig. 5. ARC inhibits ROS-induced apoptosis by blocking caspase-2 activation and Bax translocation. **A**: Caspase activation: H9c2 cells stably transfected with vector, siRNA-rARC (si3), ARC (T149A), or rARC were treated with H_2O_2 for 24 h before being harvested and lysed. Caspase-2 or -3 activities were analyzed by the substrate assay with a fluorometric kit purchased from Alexis (Ac-VDVAD-AFC for caspase-2, Ac-DEVD-AFC for caspase-3). **B**: Caspase inhibitor assay: caspase inhibitors were added to the culture of different stable cell lines 2 h prior to H_2O_2 treatment. Caspase inhibitors: z-VDVAD-FMK for caspase-2, z-DEVD-FMK for caspase-3, z-LEHD-FMK as caspase-9 inhibitor, z-VAD-FMK is pan-caspase inhibitor. Cell viability was analyzed by MTT assay as described in Materials and Methods (**$P < 0.01$ between ARC and T149A, *$P < 0.05$ between ARC and vector control). **C**: Effect of inhibitor for caspase-8: z-IETD-FMK: cells were treated with 100 μM of z-IETD-FMK for 2 h before H_2O_2 treatment. **D**: Western Blot analysis of caspase-3 cleavage and Bax translocation: transfected H9c2 cells were treated with H_2O_2 for 24 h and harvested. Cells were fractionated as described in Materials and Methods. **Lanes 1** and **1′**: ARC + H_2O_2 200 μM; **lanes 2** and **2′**: ARC + H_2O_2 400 μm; **lanes 3** and **3′**: ARC (T149A) + H_2O_2 200 μM; **lanes 4** and **4′**: ARC (T149A) + H_2O_2 400 μM. Antibody specific for cleaved caspase-3 was used to detect the 19-kD band (indicated by asterisk*). **E**: FRET analysis of interaction between ARC and Bax or T149A mutant and Bax. H9c2 cells were transfected with either ARC-CFP and Bax-YFP or T149A-CFP and Bax-YFP and treated with 200 μM H_2O_2 for 12 h before fixation. FRET was examined and calculated as described in Materials and Methods section. * Indicates statistically different between treated and untreated samples ($P < 0.05$).

protein phosphatase, PP2C interacts with ARC, which may inhibit its activity through dephosphorylation. Lastly, ARC suppressed the mitochondrial-mediated intrinsic pathway by either inhibition of caspase-2 activation, blocking translocation of Bax or both, during oxidative stress-induced apoptosis.

Our attempt to inhibit the expression of ARC with siRNA did not reduce the protein expression to the level reported in other studies employing siRNA technique, including a recent publication on ARC [Nam et al., 2004]. However, we still observed significant reduction in resistance to oxidative stress-induced apoptosis in these cells. Our oligos are targeted to the 3′-UTR (untranslated region) instead of the 5′-region as described in the study published by Nam et al. [2004]. In contrast to Nam's study, we

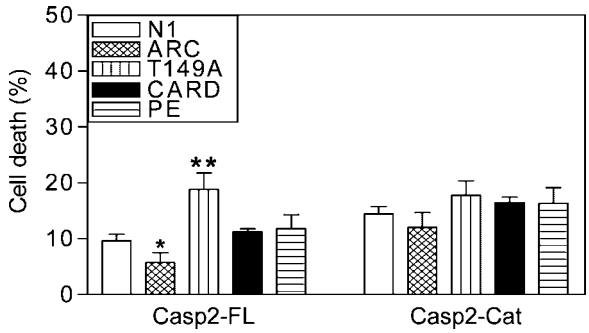

Fig. 6. ARC reduces apoptosis induced by an overexpression of caspase-2. Stable H9c2 clones with respective constructs: vector, ARC, ARC (T149A), ARC (CARD), and ARC (PE) were transfected with caspase-2 (Casp2-FL) or caspase-2 catalytic domain (Casp2-Cat) as described in Materials and Methods. Cell viability was detected by the MTT assay after 36 h of transfection (*$P < 0.001$ between T149A and other groups, *$P < 0.05$ between ARC and N1, CARD, or PE).

did not observe automatic apoptosis and Bax translocation in H9c2 cells with reduced ARC. This might be due to the difference of the degree of ARC reduction. In a separate study, ARC expression was reduced by continuously growing over-confluent H9c2 cells [Ekhterae et al., 1999]. This approach has a major drawback due to the possibility of changes in gene expression pattern and growth properties of H9c2 cells when growing in confluence for a long period [Kimes and Brandt, 1976].

For localization studies, we had to rely on the expression of fluorescent ARC fusion proteins due to the lack of a good anti-ARC antibody that could be used for immunofluorescence staining. Even though we tried many times, we found the commercially available anti-ARC antibody is not suitable for immunostaining. To confirm the results observed with the fluorescent ARC fusion protein, we used cell fractionation to analyze the distribution of ARC as well as other proteins. The combination of these two approaches provides sufficient confidence of our conclusion that wild-type ARC not T149A mutant relocalizes to mitochondria during oxidative stress.

We hypothesized that ARC might interfere with the function of the pro-apoptotic members of the bcl-2 protein family including Bax. A recent study found that indeed, ARC interacted with Bax [Gustafsson et al., 2004]. This finding is consistent with our results. Using FRET, we also found that ARC and Bax interact with each other in situ (data not shown). Overexpression of ARC blocks the translocation of Bax to mitochondria during oxidative stress-induced apoptosis (Fig. 5C). Collectively, these data indicate that inhibition of Bax translocation by ARC plays an important role in inhibiting oxidative stress-induced apoptosis.

One of the important findings in our study is that the T149A mutation has dominant negative effect against endogenous ARC, implying potential self-interaction between ARC itself. Indeed, we detected moderate interaction between ARC itself (data not shown). This appears consistent with a previous study that detected ARC interaction using the immunoprecipitation approach [Gustafsson et al., 2004]. The biological significance of this interaction has been demonstrated by our study. However, when and where the formation of ARC homodimers or homooligomers occurs requires further investigation.

Recently, the P/E rich domain of ARC was shown to be sufficient to protect against neuronal cell death [Hong et al., 2003]. However, we did not observe this same protective effect in our study. This may reflect cell specificity of ARC in terms of its anti-apoptotic function. Support for this hypothesis can be found in the results of another study from Dowds and Sabban [2001], who found that overexpression of ARC in PC12 cell, which is a neuroblastoma cell, promoted apoptosis. Thus, ARC appears to have different activities potentially in different cell types. However, our data demonstrating an anti-apoptotic effect for ARC is consistent with the bulk of the published data on ARC function.

IAPs are a family of proteins that inhibit the activation or activity of caspases [Andersen et al., 2005]. Various studies have suggested potential clinical implications for this group of proteins. For instance, some apoptosis inhibitors might help prevent or slow down degenerative disorders or autoimmune diseases. As an apoptosis inhibitor, ARC may be considered a special type of IAP. It may have the same or even more potential in preventing cell damage than other IAPs due to its pleiotropic effect in inhibiting apoptosis. The data in this study confirms that ARC is important in protecting heart cells against oxidative stress-induced damage. This aspect potentially has an important clinical implications including the prevention of damage caused by ischemia/reperfusion and hypoxia, which is associated partially with oxidative stress [Aronis et al.,

2005]. In fact, expression of ARC has been shown to reduce this type of damage in one animal study [Gustafsson et al., 2002]. Our data further identify and confirm the mechanism of how ARC prevents oxidative damage and supports the notion that high level of ARC plays a critical role in protecting heart cells from oxidative stress-induced damage. Further studies are necessary to distinguish the interaction between ARC and Bax or ARC and caspase-2/8. Since it is a pleiotropic inhibitor of caspases, ARC may have a wide spectrum of clinical implications in cell death prevention. More studies are required to investigate and compare the function of ARC in other stress-induced and/or receptor-mediated apoptosis. Furthermore, studies employing protein/peptide delivery system in animal or tissue culture to examine the role of ARC could reveal more information about the practical application of ARC as a special type of IAP.

ACKNOWLEDGMENTS

This research was supported by NIH grant AG20210 to B.H. Y-Q.Z. is a recipient of NIA training grant AG021890 directed by Dr. Olivia M. Pereira-Smith. We thank Dr. Vickie Frolick for assisting image processing. All the fluorescent images were processed in the imaging core facility of the University of Texas HSC at San Antonio.

REFERENCES

Andersen MH, Becker JC, Straten P. 2005. Regulators of apoptosis: Suitable targets for immune therapy of cancer. Nat Rev Drug Discov 4:399–409.

Araya R, Uehara T, Nomura Y. 1998. Hypoxia induces apoptosis in human neuroblastoma SK-N-MC cells by caspase activation accompanying cytochrome c release from mitochondria. FEBS Lett 439:168–172.

Aronis A, Madar Z, Tirosh O. 2005. Mechanism underlying oxidative stress-mediated lipotoxicity: Exposure of J774.2 macrophages to triacylglycerols facilitates mitochondrial reactive oxygen species production and cellular necrosis. Free Radic Biol Med 38:1221–1230.

Baliga BC, Read SH, Kumar S. 2004. The biochemical mechanism of caspase-2 activation. Cell Death Differ 11:1234–1241.

Chen X, Liang H, Van Remmen H, Vijg J, Richardson A. 2004. Catalase transgenic mice: Characterization and sensitivity to oxidative stress. Arch Biochem Biophys 422:197–210.

Deveraux QL, Reed JC. 1999. IAP family proteins—Suppressors of apoptosis. Genes Dev 13:239–252.

Deveraux QL, Stennicke HR, Salvesen GS, Reed JC. 1999. Endogenous inhibitors of caspases. J Clin Immunol 19: 388–398.

Dowds TA, Sabban EL. 2001. Endogenous and exogenous ARC in serum withdrawal mediated PC12 cell apoptosis: A new pro-apoptotic role for ARC. Cell Death Differ 8: 640–648.

Ekhterae D, Lin Z, Lundberg MS, Crow MT, Brosius FC III, Nunez G. 1999. ARC inhibits cytochrome c release from mitochondria and protects against hypoxia-induced apoptosis in heart-derived H9c2 cells. Circ Res 85:e70–e77.

Flajolet M, Rakhilin S, Wang H, Starkova N, Nuangchamnong N, Nairn AC, Greengard P. 2003. Protein phosphatase 2C binds selectively to and dephosphorylates metabotropic glutamate receptor 3. Proc Natl Acad Sci USA 100:16006–16011.

Fliss H, Gattinger D. 1996. Apoptosis in ischemic and reperfused rat myocardium. Circ Res 79:949–956.

Gao Z, Shao Y, Jiang X. 2005. Essential roles of the Bcl-2 family of proteins in caspase-2-induced apoptosis. J Biol Chem 280:38271–38275.

Gustafsson AB, Sayen MR, Williams SD, Crow MT, Gottlieb RA. 2002. TAT protein transduction into isolated perfused hearts: TAT-apoptosis repressor with caspase recruitment domain is cardioprotective. Circulation 106:735–739.

Gustafsson AB, Tsai JG, Logue SE, Crow MT, Gottlieb RA. 2004. Apoptosis repressor with caspase recruitment domain protects against cell death by interfering with Bax activation. J Biol Chem 279:21233–21238.

Herman B, Krishnan RV, Centonze VE. 2004. Microscopic analysis of fluorescence resonance energy transfer (FRET). Methods Mol Biol 261:351–370.

Holly TA, Drincic A, Byun Y, Nakamura S, Harris K, Klocke FJ, Cryns VL. 1999. Caspase inhibition reduces myocyte cell death induced by myocardial ischemia and reperfusion in vivo. J Mol Cell Cardiol 31:1709–1715.

Hong YM, Jo DG, Lee JY, Chang JW, Nam JH, Noh JY, Koh JY, Jung YK. 2003. Down-regulation of ARC contributes to vulnerability of hippocampal neurons to ischemia/hypoxia. FEBS Lett 543:170–173.

Kimes BW, Brandt BL. 1976. Properties of a clonal muscle cell line from rat heart. Exp Cell Res 98:367–381.

Koseki T, Inohara N, Chen S, Nunez G. 1998. ARC, an inhibitor of apoptosis expressed in skeletal muscle and heart that interacts selectively with caspases. Proc Natl Acad Sci USA 95:5156–5160.

Li PF, Li J, Muller EC, Otto A, Dietz R, von Harsdorf R. 2002. Phosphorylation by protein kinase CK2: A signaling switch for the caspase-inhibiting protein ARC. Mol Cell 10:247–258.

Lundberg KC, Szweda LI. 2004. Initiation of mitochondrial-mediated apoptosis during cardiac reperfusion. Arch Biochem Biophys 432:50–57.

McCaughan FM, Brown AL, Harrison DJ. 1994. The effect of inhibition of glutathione S-transferase P on the growth of the Jurkat human T cell line. J Pathol 172:357–362.

Mronga T, Stahnke T, Goldbaum O, Richter-Landsberg C. 2004. Mitochondrial pathway is involved in hydrogen-peroxide-induced apoptotic cell death of oligodendrocytes. Glia 46:446–455.

Nam YJ, Mani K, Ashton AW, Peng CF, Krishnamurthy B, Hayakawa Y, Lee P, Korsmeyer SJ, Kitsis RN. 2004. Inhibition of both the extrinsic and intrinsic death pathways through nonhomotypic death-fold interactions. Mol Cell 15:901–912.

Neuss M, Monticone R, Lundberg MS, Chesley AT, Fleck E, Crow MT. 2001. The apoptotic regulatory protein ARC (apoptosis repressor with caspase recruitment domain) prevents oxidant stress-mediated cell death by preserving mitochondrial function. J Biol Chem 276:33915–33922.

Nicholson DW. 2001. Apoptosis. Baiting death inhibitors. Nature 410:33–34.

Qin Y, Vanden Hoek TL, Wojcik K, Anderson T, Li CQ, Shao ZH, Becker LB, Hamann KJ. 2004. Caspase-dependent cytochrome c release and cell death in chick cardiomyocytes after simulated ischemia-reperfusion. Am J Physiol Heart Circ Physiol 286:H2280–H2286.

Ran Q, Van Remmen H, Gu M, Qi W, Roberts LJ II, Prolla T, Richardson A. 2003. Embryonic fibroblasts from Gpx4+/– mice: A novel model for studying the role of membrane peroxidation in biological processes. Free Radic Biol Med 35:1101–1109.

Ran Q, Liang H, Gu M, Qi W, Walter CA, Roberts LJ II, Herman B, Richardson A, Van Remmen H. 2004. Transgenic mice overexpressing glutathione peroxidase 4 are protected against oxidative stress-induced apoptosis. J Biol Chem 279:55137–55146.

Takahashi A, Masuda A, Sun M, Centonze VE, Herman B. 2004. Oxidative stress-induced apoptosis is associated with alterations in mitochondrial caspase activity and Bcl-2-dependent alterations in mitochondrial pH (pHm). Brain Res Bull 62:497–504.

Takeyama N, Miki S, Hirakawa A, Tanaka T. 2002. Role of the mitochondrial permeability transition and cytochrome C release in hydrogen peroxide-induced apoptosis. Exp Cell Res 274:16–24.

Tenev T, Zachariou A, Wilson R, Ditzel M, Meier P. 2005. IAPs are functionally non-equivalent and regulate effector caspases through distinct mechanisms. Nat Cell Biol 7:70–77.

Troy CM, Shelanski ML. 2003. Caspase-2 redux. Cell Death Differ 10:101–107.

Van Remmen H, Salvador C, Yang H, Huang TT, Epstein CJ, Richardson A. 1999. Characterization of the antioxidant status of the heterozygous manganese superoxide dismutase knockout mouse. Arch Biochem Biophys 363:91–97.

Van Remmen H, Williams MD, Guo Z, Estlack L, Yang H, Carlson EJ, Epstein CJ, Huang TT, Richardson A. 2001. Knockout mice heterozygous for Sod2 show alterations in cardiac mitochondrial function and apoptosis. Am J Physiol Heart Circ Physiol 281:H1422–H1432.

Zhao ZQ, Velez DA, Wang NP, Hewan-Lowe KO, Nakamura M, Guyton RA, Vinten-Johansen J. 2001. Progressively developed myocardial apoptotic cell death during late phase of reperfusion. Apoptosis 6:279–290.